

*This paper reports a study into the impact of cadmium telluride layer thickness on the effectiveness of the CdS/CdTe/Cu/Au film solar cells. The physical mechanisms have been investigated of charge transfer in the CdS/CdTe/Cu/Au solar cells, which are intended for use as a backup power source for the systems of safety and control of objects. This is important because, despite the growing popularity of solar cell application, the effectiveness of laboratory samples differs greatly from the theoretical maximum. Thus, it has been established that the optimum thickness of the base layer of film CdS/CdTe/Cu/Au SCs is 4 μm. When the thickness of the cadmium telluride layer is reduced, the effectiveness of such an assembly decreases. The decrease in efficiency occurs as a result of reducing the shunting electric resistance, increasing the density of a diode saturation current, as well as consistent electric resistance. With the increase in the thickness of the telluride layer exceeding 4 μm, there is also a decrease in the efficiency of a solar cell due to the reduced shunting resistance and the increased serial electric resistance. The deterioration of the specified light diode characteristics of CdS/CdTe/Cu/Au SCs, which occurs when the thickness of the base layer is reduced by more than 4 μm, is due to the diffusion of copper from the contact to the area of the separating barrier. The deterioration of light diode characteristics when increasing the thickness of the base layer of cadmium telluride is associated with a decrease in the positive effects of "chloride" treatment. The examined physical charge transfer mechanisms in the CdS/CdTe/Cu/Au solar cells have made it possible to establish the height of the rear potential barrier. In the samples studied, the height of the rear potential barrier is 0.3 eV. The existence of such a barrier gives rise to the thermal-emission mechanism of charge transfer in such solar cells when applying a direct offset exceeding 1 V*

**Keywords:** cadmium telluride, efficiency improvement, backup power, security and control systems, emergency

# DEVISING A TECHNIQUE TO IMPROVE THE EFFICIENCY OF CdS /CdTe /Cu /Au SOLAR CELLS INTENDED FOR USE AS A BACKUP POWER SOURCE FOR THE SYSTEMS OF SAFETY AND CONTROL OF OBJECTS

**N. Deyneko**

PhD, Associate Professor

Department of Special Chemistry and Chemical Engineering\*\*

E-mail: natalyadeyneko@gmail.com

**A. Zhuravel**

Leading Process Engineer\*\*\*

**L. Mikhailova**

PhD, Professor

Department of Electrical Technology, Electromechanics and Electrotechnics

State Agrarian and Engineering University in Podilia

Shevchenka str., 13, Kamianets-Podilsky, Ukraine, 32316

**E. Naden**

PhD\*

**A. Onyshchenko**

Doctor of Technical Sciences, Associate Professor

Department of Bridges and Tunnels

National Transport University

M. Omelianovycha-Pavlenka str., 1, Kyiv, Ukraine, 01010

**A. Savchenko**

PhD, Senior Researcher\*

**V. Strelets**

Doctor of Technical Sciences, Senior Researcher

Scientific Department on the Problems of Civil Defence, Technogenic and Ecological Safety of Research Center\*\*

**Ye. Yurevych**

Deputy Director\*\*\*

\*Department of Prevention Activities and Monitoring\*\*

\*\*National University of Civil Defence of Ukraine

Chernyshevskaya str., 94, Kharkiv, Ukraine, 61023

\*\*\*Design and Technology Institute of Micrographics

Akademika Pidhornoho lane, 1/60, Kharkiv, Ukraine, 61046

Received date 02.11.2020

Accepted date 07.12.2020

Published date 29.12.2020

Copyright © 2020, N. Deyneko, A. Zhuravel, L. Mikhailova,

E. Naden, A. Onyshchenko, A. Savchenko, V. Strelets, Ye. Yurevich

This is an open access article under the CC BY license (<http://creativecommons.org/licenses/by/4.0>)

## 1. Introduction

In recent years, there has been a significant increase in the use of security and control systems, both at high-risk

facilities and potentially hazardous sites [1]. This is due to the ever-increasing number of anthropogenic emergencies whose growth is due to both technological progress and the existence of many dangerous factors, as well as the pene-

tration of third parties into the territory of the facility [2]. Remote surveillance systems have become popular, allowing real-time monitoring of the situation over the Internet [3]. And it is not only video surveillance that has undergone a number of technological changes, the latter of which is the transition from analog video surveillance to fully digital network CCTV systems. The availability of sophisticated systems has changed since the advent of cheap microcontrollers such as Arduino, which have made it possible to introduce low-cost security systems that include most of the features present in expensive systems [4].

However, even though security and control systems consume only a small part of the total energy consumption of the facility, their uninterrupted operation is ensured by the presence of electricity in the network. Although many of them have a backup power supply in case of an emergency shutdown, as a rule, its charge is enough for no more than 24 hours [5].

Therefore, it is a relevant task to devise approaches to using photovoltaic elements as a reserve of the safety and control system in the event of a long absence of electricity supply from engineering networks. Such a system makes it possible to ensure the operation of security and control systems at remote objects where there is no electricity supply from engineering networks. However, to implement this approach, as well as employ it at a large-scale level, there should be solar cells whose weight is small, the cost is low while the efficiency is high.

---

## 2. Literature review and problem statement

---

Photovoltaic technologies are one of the most important renewable energy sources. Since the first recognition in 1839 [6], there have been numerous studies on the characteristics of photovoltaic converters. However, improving the efficiency and reducing the cost of photovoltaic technologies still require considerable effort. Solar cells based on crystalline silicon (c-Si) are known as materials in first-generation solar cells [7]. In terms of cost, performance, and manufacturability, the application of new advanced materials such as amorphous silicon (a-Si), cadmium telluride (CdTe), and diselenide of copper, indium, and gallium (CIGS) has been common in the second and third generations of solar panels. The typical conversion efficiency of the first-generation technologies is currently between 15 % and 24 %, while that of the second-generation technologies currently ranges from 7 % to 16 % [8,9]. Another important criterion for increasing demand for the use of solar cells is degradation resistance. Papers [10, 11] reported an analysis of the processes of degradation taking place in solar cells (hereinafter, SCs) based on cadmium telluride and proposed a way to restore their effectiveness. Work [12] examined the radiation resistance of CdTe solar cells with an efficiency of ~10 %, whose structure was formed on the anti-radiation glass. The authors found that in their case the main CdS/CdTe transition is easily destroyed. It is also important when using solar cells to pay attention to the possibility of arranging them on non-flat surfaces. The author of [13] studied solar cells built on flexible substrates.

Photovoltaic systems can be divided into autonomous photovoltaic systems and photovoltaic systems connected to the network [14]. Autonomous systems do not power the grid. Such systems can vary significantly in size and ap-

plication, for example, in consumer electronics and remote homes. For example, work [15] reports an experimental study of absorption refrigerators powered by solar cells. The system was tested when solar radiation changes in the range from 550 to 700 W/s of solar energy and 500 ml of water at room temperature as a cooling load. After 160 minutes, this refrigerator can maintain a temperature from 5 to 8 °C. Work [16] reported a solar LED street lighting system that employs control over constant power and dimming. The test results showed that the power of LED lamps of 18 W and 100 W could be precisely adjusted with a margin of error of 2–5 %.

The authors of [17], in order to functionally monitor the state of a driver's fatigue, effectively analyzed the features and actions of the human body. Identifying and recognizing the characteristics of the human body currently plays an important role in many applied areas, such as human observation and human interaction between applications and the computer [18–20]. Work [17] reports a system for monitoring drivers on the road, which uses a built-in onboard platform powered by solar panels. The driver's monitoring system on the road can determine the driver's mental state. The driver control function is performed using an effective method of eye detection. With the help of the driver's eye movements, recorded by a camera, one can determine the status of the driver's attention and avoid any fatigue conditions. This driver monitoring method was implemented on a low-power platform built into the car and run by a solar panel, which is another example of the use of solar panels in monitoring systems.

However, despite the growing use of solar cells as an autonomous power source, their large-scale application, including as a backup power supply to the systems of facilities safety and control, is still constrained by low efficiency.

---

## 3. The aim and objectives of the study

---

The aim of this work is to devise a technique to improve the efficiency of film CdS/CdTe/Cu/Au SCs, designed to provide backup power to the systems of facilities safety and control.

To accomplish the aim, the following tasks have been set:

- to investigate the effect of the thickness of a cadmium telluride layer on the effectiveness of film CdS/CdTe/Cu/Au SCs;
- to investigate the physical mechanisms of charge transfer in CdS/CdTe/Cu/Au SCs.

---

## 4. Materials and equipment used to produce CdS/CdTe/Cu/Au photovoltaic converters

---

The examined instrument structures with a photo-harvesting surface area of up to 2 cm<sup>2</sup> were made by thermal vacuum evaporation when using the vacuum installation UVN67 with modified internal equipment. The internal installation equipment is shown in Fig. 1.

Since one cannot fabricate, without a layer of copper, effective instrument structures, we deposited on the surface of telluride cadmium the nanoscale layer of copper with a thickness of 2 nm. Minimizing the thickness of the copper layer was aimed at increasing the degradation stability of the instrument structure.



Fig. 1. The internal installation system for spraying CdS and CdTe: 1, 2 – screens, 3 – evaporator of powdered cadmium telluride; 4 – evaporator of powdered cadmium sulfide; 5 – carousel, 6 – substrate heater, 7 – substrate holder

According to [21–25], the technology of tunnel electrode formation involves, before applying the electrode, conducting chemical etching, which forms a Te layer; the final stage is annealing, which leads to the formation of the  $Cu_{2-x}Te$  phase, which is a degenerate conductor.

### 5. Studying ways to improve the efficiency of CdS/CdTe/Cu/Au SCs designed for backup power

#### 5.1. Studying the effect of the thickness of a cadmium telluride layer on the effectiveness of CdS/CdTe/Cu/Au SCs

Photovoltaic conversion of solar energy is carried out in the basic layer of cadmium telluride. Therefore, when irradiating the surface of the layer of telluride cadmium with photons, the energy of which is greater than its width of the prohibited zone, the thickness of this base layer should ensure their effective absorption. It should also be noted that excessive growth of the thickness of the base layer leads to an increase in the consistent resistance of the instrument structure, which, under other equal conditions, reduces the efficiency of a solar element [26].

The depth of light absorption in CdTe films was determined on the basis of experimental spectral dependences of the transmission and reflection coefficients from the following ratio:

$$I(l) = I_0 R(l) [1 - \exp\{-x/l(l)\}],$$

where  $I_0$  is the intensity of radiation entering the base layer at a given wavelength;  $R(l)$  is the reflection coefficient of photons at a given wavelength;  $l(l)$  is the depth of absorption of photons at a given wavelength.

Using the experimental dependences of  $l(l)$  and the spectral distribution of the intensity of falling solar radiation  $AM_0$  and  $AM_{1.5}$ , corresponding to the SC range of photosensitivity SCs of (550–800) nm, we calculated the dependence of the relative cumulative absorption of light on the thickness of a cadmium telluride layer (Fig. 2). The analysis shows that the optimum thickness of the CdS/CdTe-based base layer of film SCs should be about 1  $\mu m$ . Indeed, with the increase in the thickness of the CdTe layer from 1  $\mu m$  to 2.5  $\mu m$ , the absorption of light increases by only 10 %; at the same time, the growth in the electric resistance of the base layer adversely affects the efficiency.

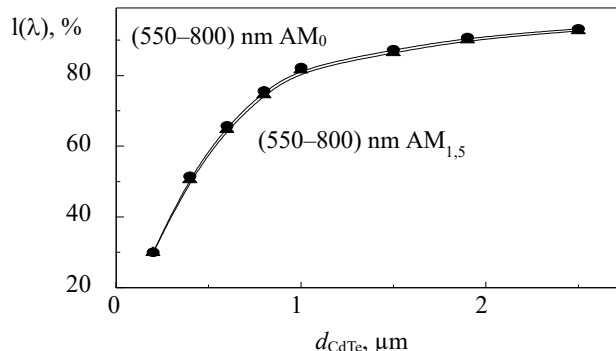


Fig. 2. Dependence of the relative integrated absorption of light on the thickness of the base layer of cadmium telluride

The CdS/CdTe/Cu/Au SCs light current-voltage characteristic measurements were carried out with the different thicknesses of a cadmium telluride layer (Fig. 3).

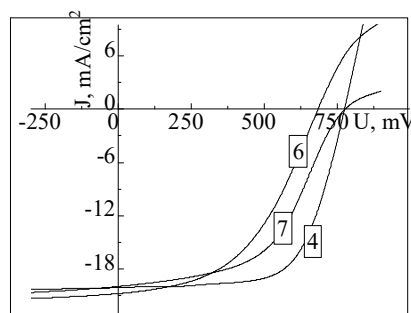


Fig. 3. Effect of the cadmium telluride layer thickness on the CdS/CdTe/Cu/Au SCs light current-voltage characteristic: 6 –  $d_{CdTe}=3 \mu m$ , 4 –  $d_{CdTe}=4 \mu m$ , 7 –  $d_{CdTe}=5 \mu m$

The thickness of a cadmium telluride layer ( $d_{CdTe}$ ) ranged from 1  $\mu m$  to 5  $\mu m$ . The thickness of a cadmium sulfide layer and a cadmium chloride layer was unchanged and amounted to 0.4  $\mu m$  and 0.35  $\mu m$ , respectively. Based on the dependence of the CdS/CdTe/Cu/Au SCs effectiveness on light diode characteristics, several characteristic ranges of cadmium telluride thickness can be identified. The effectiveness, output parameters, and the light diode characteristics of the samples that correspond to these ranges are given in Table 1.

Table 1

Effect of the cadmium telluride layer thickness on the output parameters and light diode characteristics of CdS/CdTe/Cu/Au SCs

$d_{CdTe}, \mu m$	3	4	5
$V_{oc}, mV$	682	774	757
$J_{sc}, mA/cm^2$	20.8	20.1	19.8
$FF, \text{relative units}$	0.48	0.66	0.53
$h, \%$	6.9	10.3	7.95
$R_s, \text{Ohm} \times \text{cm}^2$	7.4	2.8	8.1
$R_{sh}, \text{Ohm} \times \text{cm}^2$	127	954	240
$J_0, A/cm^2$	$1.6 \times 10^{-6}$	$5.7 \times 10^{-8}$	$5.8 \times 10^{-8}$
$A, \text{relative units}$	2.7	2.3	2.2
$J_{ph}, mA/cm^2$	21.0	20.2	20.2

Our analysis of Table 1 shows that the growth in a CdTe layer thickness from 4  $\mu m$  to 5  $\mu m$  leads to a decrease in SCs efficiency by reducing idle voltage and the fill factor of light

current-voltage characteristic. We determined the initial parameters and light diode characteristics of photovoltaic converters based on cadmium telluride according to the experimental light volt-ampere characteristics. The analytical treatment of light current-voltage characteristic of the examined SC was carried out on PC. The relationship between the SC effectiveness and the light diode characteristics is described implicitly by the theoretical light SC current-voltage characteristic:

$$J_l = -J_{ph} + J_0 \left\{ \exp \left[ \frac{e(V_l - J_l R_s)}{AkT} \right] - 1 \right\} + (V_l - J_l R_s) / R_{sh}, \tag{1}$$

where  $J_l$  is the density of the current flowing through the load,  $e$  is the electron charge;  $k$  is the Boltzmann constant,  $T$  is the temperature of the solar element;  $V_l$  is the voltage drop at loading.

Analytical expression (1) for light current-voltage characteristic is converted to expressions that take the following form:

$$I_l = A_0 - A_1 V_l - A_2 \exp(A_3 V_l + A_4 I_l), \tag{2}$$

$$A_0 = (I_{ph} + I_0) R_{st} / (R_s + R_{st}), \tag{3}$$

$$A_1 = 1 / (R_s + R_{st}), \tag{4}$$

$$A_2 = I_0 R_{st} / (R_s + R_{st}), \tag{5}$$

$$A_3 = e / (AkT), \tag{6}$$

$$A_4 = e R_s / (AkT). \tag{7}$$

Using expression (2) and experimentally derived values of  $I_l$  and  $V_l$ , by varying the values of the above-specified coefficients  $A_0, A_1, A_2, A_3, A_4$ , one achieves the best approximation of the experimental data  $I_l = I_l(V_l)$  for the curve that is described by the transformed theoretical expression (2). Typically, at analytical processing, a standard deviation does not exceed  $10^{-8}$ , which corresponds to the relative error in determining the initial parameters and the light diode characteristics at the level not larger than 1%. Upon finding the specified coefficients, which ensure the best approximation, one determines the initial parameters for PEC:  $I_{sc}, V_{oc}, FF, P_{nm}$ , efficiency. Light-emitting diode characteristics  $R_s, R_{sh}, A$  and  $I_0$  are calculated based on the derived coefficients  $A_0, A_1, A_2, A_3, A_4$  applying ratios (3) to (7) [15–17]. Error in determining the initial parameters and the light diode characteristics is defined not only by the magnitude of a standard deviation, but by the error in measuring light VAC as well.

Our numerical modeling (Fig. 3, *a, b*) has shown that the decisive impact on the reduction of SC efficiency is almost equally exerted by the reduced  $R_{sh}$  and the increased  $R_s$ . It is well-known that the mandatory manufacturing operation when making effective SCs based on CdS/CdTe is “chloride” treatment [27], which improves efficiency by several times. The result of such treatment is the decreased specific CdTe electric resistance due to the generation of  $Cl_{Te}-V_{Cd}$  acceptors with a concentration at the order of  $10^{14} \text{ cm}^{-3}$ , which reduces  $R_s$ . In addition, under such treatment, there is a re-crystallization of the base layer, in which the column structure of CdTe with small grain size is transformed into a structure of free orientation with large grain sizes. As a result, the probability of partial shunting of the separating

barrier with a grain-bearing surface decreases, causing the growth of  $R_{sh}$ . Thus, increasing the thickness of a CdTe layer at the unchanging thickness of the  $CdCl_2$  layer leads to that the described positive effect of “chloride” treatment is not fully manifested.

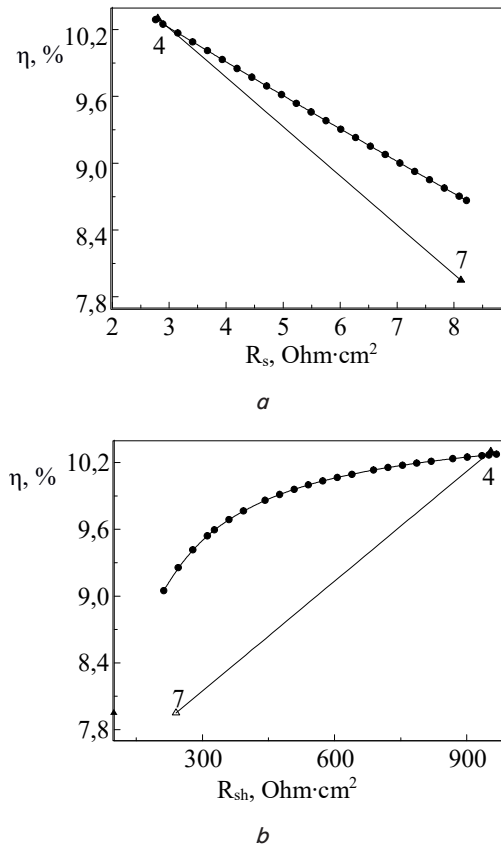


Fig. 4. Modeling the effect of change in the light diode characteristics on a change in efficiency when increasing the thickness of a CdTe layer from 4 μm to 5 μm: *a* – the dependence of efficiency on consistent resistance; *b* – the dependence of efficiency on shunt resistance; • – theoretical efficiency; ▲ – experimental efficiency

The analysis of the output parameters and light diode characteristics from Table 1 shows that reducing the thickness of a CdTe layer from 4 μm to 3 μm leads to a decrease in SC efficiency due to the reduction in  $V_{oc}$  and FF. Our numerical modeling has shown that the decisive impact on the reduction of efficiency is exerted by the growth in  $J_0$  and the decrease in  $R_{sh}$ . At the same time, the noticeable impact is due to the growth in  $R_s$ .

### 5. 2. Studying the physical mechanisms of charge transfer in CdS/CdTe/Cu/Au SCs

We studied the dark current-voltage characteristic to investigate the physical mechanisms of influence exerted by the rear contacts on SC efficiency. Typical dark current-voltage characteristic of the examined CdS/CdTe/Cu/Au SCs at direct offset are shown in Fig. 5, *a*. The analytical treatment of the experimental dark current-voltage characteristic indicates the linearization of the temperature dependence of the density of dark diode saturation current ( $J_{sc}$ ) in the  $\lg J_{sc} - 1000/T$  coordinates at a direct offset to (0.6–0.8) V (Fig. 5, *b*).



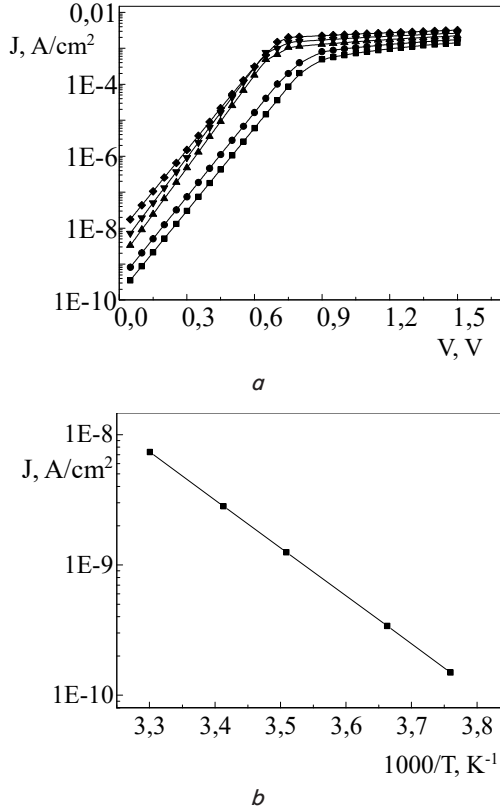


Fig. 5. Studying the electrical properties of CdS/CdTe/Cu/Au SCs:  $a$  – dark current-voltage characteristic acquired at different temperatures:  $\blacklozenge$  –  $T=30$  °C  $\blacktriangleright$  –  $T=20$  °C;  $\blacktriangle$  –  $T=12$  °C;  $\bullet$  –  $T=0$  °C;  $\blacksquare$  –  $T=-7$  °C;  $b$  – the temperature dependence of dark diode saturation current

This is the proof that the manufactured film CdS/CdTe/Cu/Au SCs at these direct offsets implement a thermally activated recombination charge transfer mechanism, in which dark current-voltage characteristic can be modeled with the following theoretical expressions:

$$J = J_{sc} \{ \exp(eV/AkT) - 1 \}, \quad (8)$$

where  $J_{sc}$  is the density of dark diode saturation current,  $V$  is the voltage;  $e$  is the electron charge;  $A$  is the perfection coefficient;  $k$  is the Boltzmann constant;  $T$  is the temperature.

$$J_{sc} = J_{so} \exp(-E_a/kT), \quad (9)$$

where  $E_a$  is the saturation current activation energy associated with the height of a potential barrier ( $E_b$ ) via the ratio  $E_a = E_b/A$ .

The analytical treatment of the experimental dependences  $J$  ( $1/T$ ) shows that the activation energy of CdS/CdTe/Cu/Au SCs charge transfer is 0.75 eV. Taking into consideration the fact that the dark perfection factor of the examined CdS/CdTe/Cu/Au SCs accepts a value of 1.9, we obtain  $E_b = 1.43$  eV. The theoretical value of the height of the potential barrier of the  $p$ CdS- $n$ CdTe heterojunction differs significantly from the experimental value of  $E_b = 1.43$  eV because, according to literary data [25], it is 1.02 eV. The width of the prohibited zone of the film layers of cadmium telluride is 1.46 eV. Given this, we can conclude that in the examined

SCs the division of charge carriers is enabled by the  $p$ - $n$  junction, which is formed in the base layer of  $p$ -CdTe. At the same time, according to the experimental data obtained from the elemental analysis and optical research, a layer of the  $n$ -type electrical conductivity may be the variance layers of the CdS<sub>x</sub>Te<sub>1-x</sub> solid solutions. Thus, the formation of the CdS<sub>x</sub>Te<sub>1-x</sub> solid solutions not only reduces the difference in the lattice periods of telluride and cadmium sulfide but it also shifts the region of the built-in electric field away from the CdS-CdTe interphase boundary deep into the base layer of cadmium telluride as a result of the formation of the  $n$ CdS<sub>x</sub>Te<sub>1-x</sub>- $p$ CdTe heterojunction. In such a transition in the examined SCs it carries out the division of uneven charge carriers. At the same time, the negative impact of the surface recombination on the diode characteristics of the separating barrier decreases.

At large direct offsets ( $V > 1$  V), the shape of the examined SC current-voltage characteristic is affected by the rear contact. To describe the features of charge transfer in CdS/CdTe/Cu/Au SCs at direct offsets over 1 V, it was suggested to take into consideration the rear contact as a consistently connected diode. In this case, the rear contact, which, together with the base layer of cadmium telluride, forms the Schottky barrier, is connected in a direction opposite to the main  $p$ - $n$  transition. Our study has shown that the dark current-voltage characteristic of CdS/CdTe/Cu/Au SCs demonstrates a plateau under a voltage exceeding 1 V. At the same time, the amount of current density corresponding to the plateau increases with the temperature rise. Thus, the density of the current passing SCs is limited to the density of the saturation current of the rear contact ( $J_1$ ). In this case,

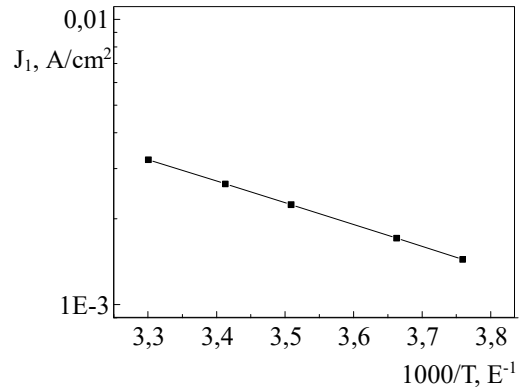


Fig. 6. Saturation current temperature dependence for CdS/CdTe/Cu/Au SCs in the  $\lg J_1 - 1000/T$  coordinates

in the  $\lg J_1 - 1000/T$  coordinates, there is a linearization of the experimental dependence  $J_1(T)$  (Fig. 6).

This indicates that at direct shifts exceeding 1 V there is a thermal-emission charge transfer mechanism acting in the CdS/CdTe/Cu/Au instrument structure:

$$J_1 \sim \exp(-E_{ac}/kT), \quad (10)$$

where  $E_{ac}$  is the energy of activation of the saturation current of the rear contact, which is correspondingly related to the height of the potential rear contact barrier ( $E_{bc}$ ) via the ratio  $E_{ac} = E_{bc}/A$ .

For the examined CdS/CdTe/Cu/Au SCs, the  $E_{ac}$  value is 0.16 eV;  $A = 1.9$ , and, therefore,  $E_{bc} = 0.30$  eV. The resulting value is practically the same as  $E_{bc} = (0.31 - 0.33)$  eV, certain

for the film CdS/CdTe/Cu/Au SCs made by physical vacuum evaporation.

### 5. Discussion of results of studying the effectiveness and physical mechanisms of charge transfer in the film CdS/CdTe/Cu/Au SCs

According to earlier studies [10, 11], in the film ITO/CdS/CdTe/Cu/Au SCs the main mechanism of degradation in their efficiency is associated with a copper diffusion into the CdS/CdTe heterojunction region from a Cu/Au electrode. This process causes a decrease in the quality of the separating barrier by increasing the density of the diode saturation current and reducing the shunting electric resistance. The analysis of the dependence of relative integrated light absorption on the thickness of a cadmium telluride layer (Fig. 2) shows that the optimum thickness of the CdS/CdTe-based base layer of film SCs should be about 1  $\mu\text{m}$ .

When the thickness of a CdTe layer increases from 1  $\mu\text{m}$  to 2.5  $\mu\text{m}$ , the absorption of light increases. However, with the thickness of a CdTe layer of 3  $\mu\text{m}$ , copper diffusion is observed in the CdS/CdTe heterojunction area from the Cu/Au electrode, causing a decrease in the quality of the separating barrier by increasing the density of the diode saturation current and reducing the shunting electric resistance (Table 1). Our modeling of the effect of change in the light diode characteristics on a change in efficiency when increasing the thickness of a CdTe layer from 4  $\mu\text{m}$  to 5  $\mu\text{m}$  has made it possible to establish that increasing the thickness of a CdTe layer from 4  $\mu\text{m}$  to 5  $\mu\text{m}$  reduces the shunting electric resistance ( $R_{sh} = 954 \text{ Ohm}\cdot\text{cm}^2$  for  $d_{\text{CdTe}} = 4 \mu\text{m}$ , and  $R_{sh} = 240 \text{ Ohm}\cdot\text{cm}^2$  for  $d_{\text{CdTe}} = 5 \mu\text{m}$ ) and increases sequential resistance ( $R_s = 2.8 \text{ Ohm}\cdot\text{cm}^2$  for  $d_{\text{CdTe}} = 4 \mu\text{m}$ , and  $R_s = 8.1 \text{ Ohm}\cdot\text{cm}^2$  for  $d_{\text{CdTe}} = 5 \mu\text{m}$ ). This, in turn, affects the reduction of idle voltage and the fill factor of the light volt-ampere characteristic (Table 1). Thus, the optimum thickness of the basic layer of film CdS/CdTe/Cu/Au SCs is 4  $\mu\text{m}$  (Table 1), which makes it possible to ensure the effective absorption of solar radiation and neutralizes the impact of the Cu/Au rear contact on the quality of the main separating barrier.

Our study of the physical mechanisms of charge transfer in the film CdS/CdTe/Cu/Au SCs suggests the following physical mechanisms that form the rear contacts in the examined CdS/CdTe/Cu/Au SCs. For SCs, after etching the

cadmium telluride layer in a solution of bromine in methanol, a layer of amorphous tellurium with a thickness of 2–3 nm is formed on the surface of the base layer. The etching is carried out in accordance with the  $\text{CdTe (solid)} + \text{Br}_2 (\text{CH}_3\text{OH}) (\text{liquid}) = \text{Te (solid)} + \text{CdBr}_2 (\text{liquid}) + \text{CH}_3\text{OH (liquid)}$  chemical reaction. The layer of the amorphous tellurium is characterized by low electrical conductivity.

For SC with a rear Cu/Au contact, the annealing of the formed CdS/CdTe/Cu/Au structure in the air at 200 °C causes the formation of a  $p+\text{Cu}_x\text{Te}$ -type connection on the surface of the base layer. Such a connection is a degenerated semiconductor with a significantly higher electrical conductivity compared to crystalline tellurium. Diffusing into the base layer at SC annealing, copper atoms generate acceptor levels within it. Both specified factors predetermine the formation of a Cu- $p$ +CdTe tunnel contact with a low contact electric resistance. That makes it possible to use relatively cheap Cu/Au materials, compared to platinum, to construct tunnel contacts for efficient CdS/CdTe-based solar cells.

### 6. Conclusions

1. It has been established that the optimum thickness of the base layer of the film CdS/CdTe/Cu/Au SCs is 4  $\mu\text{m}$ . When the thickness of cadmium telluride decreases, the efficiency of such an instrumental structure decreases. This occurs as a result of reducing the shunting electric resistance, increasing the density of the diode saturation current, and consistent electric resistance. With the increase in the thickness of cadmium telluride, the efficiency is reduced by reducing the shunting electric resistance and increasing the consistent electric resistance.

When the thickness of the base layer is reduced from the optimum value, the deterioration of the specified light diode characteristics of ITO/CdS/CdTe/Cu/Au SCs is due to the diffusion of copper from the contact to the region of the separating barrier. When increasing the thickness of the base layer, the deterioration of light diode characteristics is associated with a decrease in the positive effect of “chloride” treatment.

2. We have established that the height of the rear potential barrier in the CdS/CdTe/Cu/Au SCs is 0.3 eV. The presence of this barrier gives rise to the thermal-emission mechanism of charge transfer in such SCs when applying a direct offset exceeding 1 V.

### References

1. CHEMICAL SECURITY. DHS Could Use Available Data to Better Plan Outreach to Facilities Excluded from Anti-Terrorism Standards. GAO-20-722. Available at: <https://www.gao.gov/assets/710/709739.pdf>
2. Webb, R. (2019). Warehouse Risk Management: Is Your Facility Secure? ClearRisk. Available at: <https://www.clearrisk.com/risk-management-blog/is-your-warehouse-secure>
3. Patru, G.-C., Tranca, D.-C., Costea, C.-M., Rosner, D., Rughinis, R.-V. (2019). LoRA based, low power remote monitoring and control solution for Industry 4.0 factories and facilities. 2019 18th RoEduNet Conference: Networking in Education and Research (RoEduNet). doi: <https://doi.org/10.1109/roedunet.2019.8909499>
4. Gaol, F. L., Soewito, B. (2015). Selected Peer-Reviewed Articles from the 3rd International Conference on Internet Services Technology and Information Engineering 2015 (ISTIE 2015), Discovery Kartika Plaza Hotel, Kuta, Bali, Indonesia, 30–31 May, 2015. Advanced Science Letters, 21 (10), 2947–2951. doi: <https://doi.org/10.1166/asl.2015.6431>
5. Stallings, W. (2017). Physical Security Essentials. Computer and Information Security Handbook, 965–979. doi: <https://doi.org/10.1016/b978-0-12-803843-7.00069-7>
6. Yang, D., Yin, H. (2011). Energy Conversion Efficiency of a Novel Hybrid Solar System for Photovoltaic, Thermoelectric, and Heat Utilization. IEEE Transactions on Energy Conversion, 26 (2), 662–670. doi: <https://doi.org/10.1109/tec.2011.2112363>

7. Gaur, A., Tiwari, G. N. (2013). Performance of Photovoltaic Modules of Different Solar Cells. *Journal of Solar Energy*, 2013, 1–13. doi: <https://doi.org/10.1155/2013/734581>
8. Van de Kaa, G., Rezaei, J., Kamp, L., de Winter, A. (2014). Photovoltaic technology selection: A fuzzy MCDM approach. *Renewable and Sustainable Energy Reviews*, 32, 662–670. doi: <https://doi.org/10.1016/j.rser.2014.01.044>
9. Khrypunov, G., Vambol, S., Deyneko, N., Sychikova, Y. (2016). Increasing the efficiency of film solar cells based on cadmium telluride. *Eastern-European Journal of Enterprise Technologies*, 6 (5 (84)), 12–18. doi: <https://doi.org/10.15587/1729-4061.2016.85617>
10. Bolbas, O., Deyneko, N., Yeremenko, S., Kyrylova, O., Myrgorod, O., Soshinsky, O. et. al. (2019). Degradation of CdTe SC during operation: modeling and experiment. *Eastern-European Journal of Enterprise Technologies*, 6 (12 (102)), 46–51. doi: <https://doi.org/10.15587/1729-4061.2019.185628>
11. Deyneko, N., Kovalev, P., Semkiv, O., Khmyrov, I., Shevchenko, R. (2019). Development of a technique for restoring the efficiency of film ITO/CdS/CdTe/Cu/Au SCs after degradation. *Eastern-European Journal of Enterprise Technologies*, 1 (5 (97)), 6–12. doi: <https://doi.org/10.15587/1729-4061.2019.156565>
12. Guanggen, Z., Jingquan, Z., Xulin, H., Bing, L., Lili, W., Lianghuan, F. (2013). The effect of irradiation on the mechanism of charge transport of CdTe solar cell. 2013 IEEE 39th Photovoltaic Specialists Conference (PVSC). doi: <https://doi.org/10.1109/pvsc.2013.6745054>
13. Deyneko, N. (2020). Study of Methods for Producing Flexible Solar Cells for Energy Supply of Emergency Source Control. *Materials Science Forum*, 1006, 267–272. doi: <https://doi.org/10.4028/www.scientific.net/msf.1006.267>
14. Singh, G. K. (2013). Solar power generation by PV (photovoltaic) technology: A review. *Energy*, 53, 1–13. doi: <https://doi.org/10.1016/j.energy.2013.02.057>
15. Chien, Z.-J., Cho, H.-P., Jwo, C.-S., Chien, C.-C., Chen, S.-L., Chen, Y.-L. (2013). Experimental Investigation on an Absorption Refrigerator Driven by Solar Cells. *International Journal of Photoenergy*, 2013, 1–6. doi: <https://doi.org/10.1155/2013/490124>
16. Huang, B.-J., Chen, C.-W., Hsu, P.-C., Tseng, W.-M., Wu, M.-S. (2012). Direct battery-driven solar LED lighting using constant-power control. *Solar Energy*, 86 (11), 3250–3259. doi: <https://doi.org/10.1016/j.solener.2012.07.028>
17. Chen, Y.-L., Yu, C.-W., Chien, Z.-J., Liu, C.-H., Chiang, H.-H. (2014). On-Road Driver Monitoring System Based on a Solar-Powered In-Vehicle Embedded Platform. *International Journal of Photoenergy*, 2014, 1–12. doi: <https://doi.org/10.1155/2014/309578>
18. Moeslund, T. B., Hilton, A., Krüger, V. (2006). A survey of advances in vision-based human motion capture and analysis. *Computer Vision and Image Understanding*, 104 (2-3), 90–126. doi: <https://doi.org/10.1016/j.cviu.2006.08.002>
19. Haritaoglu, I., Harwood, D., Davis, L. S. (2000). W/sup 4/: real-time surveillance of people and their activities. *IEEE Transactions on Pattern Analysis and Machine Intelligence*, 22 (8), 809–830. doi: <https://doi.org/10.1109/34.868683>
20. Turk, M. (2004). Computervision in the interface. *Communications of the ACM*, 47 (1), 60. doi: <https://doi.org/10.1145/962081.962107>
21. Mamazza, R., Balasubramanian, U., More, D. L., Ferekides, C. S. (2002). Thin films of CdIn/sub 2/O/sub 4/ as transparent conducting oxides. *Conference Record of the Twenty-Ninth IEEE Photovoltaic Specialists Conference*, 2002. doi: <https://doi.org/10.1109/pvsc.2002.1190640>
22. Minami, T., Kakumu, T., Takeda, Y., Takata, S. (1996). Highly transparent and conductive ZnO In<sub>2</sub>O<sub>3</sub> thin films prepared by d.c. magnetron sputtering. *Thin Solid Films*, 290-291, 1–5. doi: [https://doi.org/10.1016/s0040-6090\(96\)09094-3](https://doi.org/10.1016/s0040-6090(96)09094-3)
23. Venkatesan, M., McGee, S., Mitra, U. (1989). Indium tin oxide thin films for metallization in microelectronic devices. *Thin Solid Films*, 170 (2), 151–162. doi: [https://doi.org/10.1016/0040-6090\(89\)90719-0](https://doi.org/10.1016/0040-6090(89)90719-0)
24. Jeong, W.-J., Park, G.-C. (2001). Electrical and optical properties of ZnO thin film as a function of deposition parameters. *Solar Energy Materials and Solar Cells*, 65 (1-4), 37–45. doi: [https://doi.org/10.1016/s0927-0248\(00\)00075-1](https://doi.org/10.1016/s0927-0248(00)00075-1)
25. Meriuts, A. V., Khrypunov, G. S., Shelest, T. N., Deyneko, N. V. (2010). Features of the light current-voltage characteristics of bifacial solar cells based on thin CdTe layers. *Semiconductors*, 44 (6), 801–804. doi: <https://doi.org/10.1134/s1063782610060187>
26. Khrypunov, G. S., Chernykh, E. P., Kovtun, N. A., Belonogov, E. K. (2009). Flexible solar cells based on cadmium sulfide and telluride. *Semiconductors*, 43 (8), 1046–1051. doi: <https://doi.org/10.1134/s1063782609080156>
27. Boyko, B. T., Khrypunov, G. S., Meriuts, A. V., Chernykh, O. P. (2005). The Investigation ITO/Cds/CdTe/Cu/Au Thin Film Solar Cells. *Physics and chemistry of solid state*, 6 (2), 295–298.